Data-driven Targeted Advertising Recommendation System for Outdoor Billboard

LIANG WANG, ZHIWEN YU, and BIN GUO, Northwestern Polytechnical University, China
DINGQI YANG, University of Macau, China
LIANBO MA, Northeastern University, China
ZHIDAN LIU, Shenzhen University, China
FEI XIONG, Beijing Jiaotong University, China

In this article, we propose and study a novel data-driven framework for Targeted Outdoor Advertising Recommendation (TOAR) with a special consideration of user profiles and advertisement topics. Given an advertisement query and a set of outdoor billboards with different spatial locations and rental prices, our goal is to find a subset of billboards, such that the total targeted influence is maximum under a limited budget constraint. To achieve this goal, we are facing two challenges: (1) it is difficult to estimate targeted advertising influence in physical world; (2) due to NP hardness, many common search techniques fail to provide a satisfied solution with an acceptable time, especially for large-scale problem settings. Taking into account the exposure strength, advertisement matching degree, and advertising repetition effect, we first build a targeted influence model that can characterize that the advertising influence spreads along with users mobility. Subsequently, based on a divide-and-conquer strategy, we develop two effective approaches, i.e., a master–slave-based sequential optimization method, TOAR-MSS, and a cooperative co-evolution-based optimization method, TOAR-CC, to solve our studied problem. Extensive experiments on two real-world datasets clearly validate the effectiveness and efficiency of our proposed approaches.

CCS Concepts: • **Information systems → Information systems applications;**

Additional Key Words and Phrases: Influence spread, outdoor advertising, graph model, large-scale optimization

ACM Reference format:
Liang Wang, Zhiwen Yu, Bin Guo, Dingqi Yang, Lianbo Ma, Zhidan Liu, and Fei Xiong. 2022. Data-driven Targeted Advertising Recommendation System for Outdoor Billboard. *ACM Trans. Intell. Syst. Technol.* 13, 2, Article 29 (January 2022), 23 pages.
https://doi.org/10.1145/3495159

This work is supported by the National Key Research and Development Program of China (No. 2018YFB2100800), the National Natural Science Foundation of China (No. U2001207, 61972319, 61872033), the Fundamental Research Funds for the Central Universities (No.31020180QD139), Beijing Nova Program (Z201100006820015) from Beijing Municipal Science and Technology Commission, University of Macau (SRG2021-00002-IOTSC) and FDCT Macau SAR (SKL-IOTSC-2021-2023).
Authors' addresses: L. Wang, Z. Yu, and B. Guo, Northwestern Polytechnical University, 127 West Youyi Rd, Xi'an, Shaan Xi, 710072, China; emails: liangwang0123@gmail.com, {zhiwenyu, guob}@nwpu.edu.cn; D. Yang, University of Macau, Avenida da Universidade, Taipa, Macau, China; email: dingqiyang@um.edu.mo; L. Ma, Northeastern University, No. 3-11, Wenhua Road, Shenyang, China; email: malb@swc.neu.edu.cn; Z. Liu, Shenzhen University, 3688 Nanhai Avenue, Shenzhen, China; email: liuzhidan@szu.edu.cn; F. Xiong, Beijing Jiaotong University, No. 3 Shangyuancun, Beijing, 100044, China; email: xiongf@bjtu.edu.cn.

2157-6904/2022/01-ART29 $15.00
https://doi.org/10.1145/3495159

1 INTRODUCTION

According to a recent market study released by Technavio,[1] the global outdoor advertising business is expected to grow to 45.46 billion dollars by 2021, at a compound annual growth rate about to 5% over a forecast period. Therein, as the most common advertising form, outdoor billboard, which focuses on delivering marketing information to users when they are in transit, takes a majority of the market share, about 66%.[2] More specifically, the statistics show that U.S. consumers are exposed to outdoor billboard ad for about 59 minutes per week. In practice, billboard advertising focuses on promoting product/service information to users when they are in transit [27].

To achieve a successful billboard advertising campaign, advertisers seek to expand marketing influence to targeted consumers with a limited promotion expenditure. First, the targeted consumers should be identified to a maximum extent. Because it brings little benefit by delivering ad content to "wrong audiences" who have no interest in the content. Fortunately, the largely available digital footprints of users enable us to create a much more precise user profile, i.e., characterizing subtly individual's interests and preferences [6, 15, 16, 28]. We conduct an empirical mobile users profiling study, exploring moving trajectories of taxicabs traveling in Chengdu, China. By extracting and analyzing the surrounding environment of each trajectory's destination, its implicit traveling intention, which would reflect the user's interest and preference, can be modeled by a distribution of topics, where the topics are constructed by applying the bag-of-words model [4] on spatial **Point of Interest (POI)** categories, e.g., scenic spot, Chinese restaurant, and so on. Practically, POI categories have been widely used to characterize users' interest and preference [5, 22]. By projecting each trip's intention to its covered road segments, the collective preferences of users can be obtained over each road segment, and associated with relative roadside facilities, e.g., outdoor billboards. As shown in the left part of Figure 1, the integrated results of users' preferences over different road segments are displayed in different colors, where a portion of POI categories are present in the right part. Intuitively, if mobile audience's intention coincides with a displayed ad content, then the return on marketing investment can be improved markedly.

After creating a user profile, we need to measure the advertising influence from billboard media to on-the-go audiences. At present, some naive tools, e.g., gross traffic volume [6, 32, 33] and detour distance [36], are employed to approximate the influence. However, such measurement suffers from the following limitations: (1) As it ignores the preference of the *targeted* audience, it is difficult to implement targeted advertising. (2) Due to the users mobility, it might repeatedly expose the audiences in the same ad information, which refers to "redundant advertising." In practice, the redundant advertising is discouraging, as it not only results in wasted advertising resources but also makes audiences bored and even irritated [2, 9]. So, it is necessary to develop a novel and tailored targeted billboard advertising influence model.

Finally, based on the desired targeted advertising influence, business people can make informed marketing decisions to promote their products/services. However, considering redundant advertising and different billboard rental prices (due to the distinct advertisement exposure opportunities), it is not trivial to accurately evaluate the correlation between targeted influence and corresponding promotion cost and to determine an optimal subset of displayed billboards under a pre-given advertising budget. To this end, we propose and study a **Targeted Outdoor Advertising Recommendation (TOAR)** problem in this article. Given an advertisement query, a set of candidate billboards and a budget, TOAR strives to effectively search a subset of billboards, such that the total targeted influence is maximized within the pre-given budget.

[1] https://www.technavio.com.
[2] http://www.prnewswire.com.

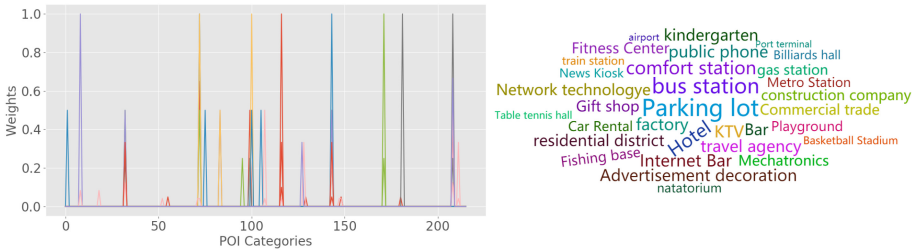

Fig. 1. The users' collective preferences over different roads.

However, to solve our studied TOAR problem, we are facing at least two challenges: (1) It is difficult to model the targeted advertising influence in the physical world, considering advertisement topics, users' preferences and the advertising repetition effect. (2) Due to the NP-hardness of the TOAR problem, common exact algorithms fail to provide a satisfied solution within an acceptable time, especially for large-scale problem settings, i.e., involving a large number of candidate billboards.

To overcome these challenges, we first build a targeted ad influence model to estimate the influence of outdoor billboard on potential audiences, by considering the impacts of advertising topic matching and the influence redundancy effect. In addition, we devise an billboard rental price mechanism from the view of advertising exposure opportunities. Subsequently, we formalize our TOAR problem and analyze its complexity. To effectively solve this problem with large-scale dimensions, based on the divide-and-conquer strategy, we develop two approaches, namely a master–slave-based sequential optimization algorithm, *TOAR-MSS*, and a cooperative co-evolution-based optimization algorithm**, TOAR-Cooperative Co-evolution (TOAR-CC)**, respectively. Specifically, we make the following contributions.

- To the best of our knowledge, this is the first work to study the problem of targeted outdoor advertising recommendation (i.e., TOAR). Compared to the existing relevant studies, TOAR takes into account of topic-aware targeted advertising and fine-grained mobility patterns.
- By utilizing the divide-and-conquer strategy, we first devise a graph-embedding-based problem decomposition method to decompose our studied problem into many smaller and simper subcomponents. Then, we propose two effective problem-solving approaches, including a master–slave-based sequential optimization algorithm, TOAR-MSS, and a cooperative co-evolution-based optimization algorithm, TOAR-CC, respectively, to tackle the TOAR problem in Section 4.
- We perform an extensive experimental study on real-world datasets, validating the performance of our proposed approaches in Section 5.

2 RELATED WORK

Influence Maximization in Geo-social Networks. Recently, by incorporating a spatial dimension, traditional **Influence Maximization (IM)** problems are extended to a location-aware scenario [11, 12, 22, 26]. Li et al. strive to search a seed set of users to maximize the influence propagation in a predefined region [11]. An influence spanning maximization problem in geo-social networks is proposed and studied in Reference [12], where the maximum geographic spanning region is identified under a constraint of predefined regional acceptance rate. Wang et al. [26] formulate a distance-aware influence maximization problem in geo-social networks and propose two novel index-based approaches to achieve online query. In Reference [22], a multi-objective

optimization-based influence spread framework is developed to reveal the full view of Pareto-optimal solutions in geo-social networks. Nevertheless, all the above research efforts focus on influence spreading over online social networks [25] instead of the physical world in our problem scenario. So it invalidates the commonly used influence propagation model, such as independent cascade, linear threshold model, and so on, and calls for novel model to accommodate our studied problem.

Trajectory-based Billboard Placement. Using a taxi GPS trajectory record, Liu et al. first study the billboard location selection problem and develop a visual analytics tool named *SmartAdP* [17]. Similarly to Reference [17], Huang et al. propose an interest-driven outdoor advertising location selection problem by leveraging mobile phone data [7]. Especially, the advertising influence is estimated as the size of covered historical trajectories in a given database. Zheng et al. [36] study a roadside advertisement dissemination research, in which the effectiveness of advertising influence is evaluated by users' detour distance. Some work study billboard advertising problems in public transportation systems, such as bus, metro, and so on [6, 31, 32]. Zhang et al. [32] study a bus/train advertisement recommendation problem in which full-wrap buses act as moving advertising mediums to influence passengers. Via capturing users' motion patterns and interests, the original problem is transformed into a top-k retrieval problem for advertisement recommendation. By maximizing a trajectory coverage for top-k bus routes, Zhang et al. further extend the above-mentioned problem in a citywide bus system [31]. Given a trajectory database, Guo et al. strive to retrieve k best trajectories to be attached with an advertisement, with the goal of maximizing the influence among a crowd of audience with certain spatio-temporal patterns [6]. Through its submodular property, greedy-based search approaches are proposed to find solutions with a constant approximation ratio.

Wang et al. [24] set up a more general scenario, where the influence is estimated by a cumulative influence probability. Zhang et al. [33] study a problem of trajectory-driven billboard placement: Given a set of billboards, a trajectory database, and a budget, it strives to find a subset of billboards under a budget constraint, such that the number of influenced trajectories is maximized. Taking into consideration impression counts, Zhang et al. extend the aforementioned work and examine a novel problem, namely ICOA [35]. Based on an integrated quantitative model, an influence maximization targeted billboard advertising problem is formulated to find k advertising units over spatiotemporal dimensions [23].

Compared with the existing research, the core differences of our TOAR problem lie in the following aspects: (1) By incorporating advertising content topics and users' preferences, we focus on targeted billboard advertising to potential customers, instead of all the mobile users; (2) different from the trajectory-coverage-based model [6, 7, 17, 33, 35] or distance-based model [24, 36], we establish a data-driven targeted ad influence spread model by comprehensively considering fine-grained mobility transition and advertising repetition effect; and (3) almost all research assumes that the billboards at different places have the same rental price [23], which is an unrealistic setting in practice. By considering relevant factors, we build an exposure-opportunity-based ad price mechanism. Therefore, we cannot directly apply the existing solutions to solve our problem.

3 PRELIMINARY AND PROBLEM DEFINITION

3.1 Targeted Billboard Advertising Influence Model

3.1.1 Individual Billboard Advertising Influence. In this work, one trajectory is characterized with a digitized timestamped sequence: $Tr = \{pt_1, pt_2, \ldots, pt_n\}$, where pt_i denotes a spatial location with time point t_i, i.e., $pt_i = (loc_i, t_i)$. By investigating Tr's destination location pt_n, its holder's preference can be profiled by the POI categories from its surroundings on the basis of the bag-of-words model [6]. Recall the Figure 1, we leverage POI categories as the vocabulary of "words." To

be specific, considering a set of POI categories $O = \{o_1, o_2, \ldots, o_m\}$, the implicit preference, i.e., traveling intention, can be represented with an empirical distribution $\overrightarrow{\eta}$ over surrounding POI categories, where $\overrightarrow{\eta} = \{\eta_1, \eta_2, \ldots, \eta_m\}$ and $\sum_{i=1}^{m} \eta_i = 1$. For example, one traveling intention can be formalized as $\{0.3, 0.7\}$ over POI categories $\{entertainment, dining\}$. Similarly, *ad query* q is also represented as $q = \overrightarrow{\gamma}$, where $\overrightarrow{\gamma} = (\gamma_1, \gamma_2, \ldots, \gamma_m)$ is q's content topic distribution over POI categories O [13]. To deliver advertisement q to on-the-go audiences, outdoor billboard media is placed at road segment $r \in \mathcal{R}$, where $\mathcal{R}$ denotes the set of candidate road segments throughout a city. Hereafter, we also use r to indicate the outdoor billboard located on r.

Without loss of generality, ad query q is assumed to be displayed on billboard r within one day. However, our outdoor advertisement influence is orthogonal to the choice of billboard display time frame. Different from the traffic volume tool, we quantify targeted advertising influence $\mathcal{I}_q^r$, i.e., billboard r's influence for q, by incorporating two key factors: *exposure strength* and *advertisement matching degree*.

(1) **Exposure Strength:** By looking into the traditional influence measurement of one of the largest outdoor advertising companies LAMAR,[3] it is observed that the panel size is used as an intuitive indicator of exposure frequency [33]. As there exists no real data, here for simplicity, we adopt a constant factor a_0 to denote the billboard size in the work. In addition, when more people coming across billboard r, more prospective audiences might be reached by q displayed on r [32]. Following this common sense, the exposure strength should also depends on two measurements: traffic flow fw and average travel speed v across billboard r. Specifically, larger fw and lower v would increase the opportunity of the displayed ad q being viewed by passerby. By traversing trajectory records $\mathcal{TB}$, we can obtain the empirical traffic flow and travel speed on each road r, i.e., $fw(r)$ and $v(r)$, respectively. And in light of traffic volume saturation [10], we comprehensively define outdoor billboard's exposure strength as follows:

$$\mathcal{H}(r) = a_0 * a_1 * log_2 fw(r) * exp(-a_2 * v(r)), \tag{1}$$

where a_0 denotes the billboard size, a_1 and a_2 are for normalizing fw and v, respectively. Obviously, the exposure strength $\mathcal{H}(r)$ is independent of ad query q.

(2) **Advertisement Matching Degree:** The advertisement matching degree is commonly used in the targeted advertising, as it is capable of capturing the potential targeted customers. The reason lies in that, audiences who are more interested in q (i.e., traveling intention matches better q) are more likely to adopt the promoted products/services. Thus, we leverage cosine similarity to evaluate the matching degree between q's content topic and the collective traveling intention over r. Formally, the matching degree can be calculated using a dot product as below:

$$Sim(q, r) = \frac{\overrightarrow{\gamma} \cdot \overrightarrow{\eta}}{\|\overrightarrow{\gamma}\| \|\overrightarrow{\eta}\|} = \frac{\sum_{i=1}^{m} \gamma_i \eta_i}{\sqrt{\sum_{i=1}^{m} \gamma_i^2} \sqrt{\sum_{i=1}^{m} \eta_i^2}}, \tag{2}$$

where $\overrightarrow{\gamma}$ denotes q's topic and $\overrightarrow{\eta}$ is the empirical traveling intention distribution over r.

So far, we formally define *targeted billboard advertising influence* for each billboard. Given ad query $q = \overrightarrow{\gamma}$, its individual targeted advertising influence $\mathcal{I}_q^r$ from billboard r can be quantified by combining both r's exposure strength and the advertisement matching degree:

$$\mathcal{I}_q^r = \mathcal{H}(r) * Sim(q, r). \tag{3}$$

[3] http://www.lamar.com.

3.1.2 Billboard Advertising Influence Diffusion Model. When q is displayed on more than one billboard, audiences may receive the same information many times in transit. In such a case, there exits *redundant advertising* to audiences as mentioned above [33]. In other words, advertising influence from each billboard can disseminate to elsewhere along with users' mobility. So, given a subset of determined billboards $\mathcal{R}^* \subseteq \mathcal{R}$, the total advertising influence should not be a simple summation of all the involved billboards' individual influence, such as $\sum_{r \in \mathcal{R}^*} \mathcal{I}_q^r$, but should rather consider the redundant advertising effect. By means of user mobility transition, we design a billboard advertising influence diffusion model to characterize redundant advertising effect.

First, we compute mobility transition probabilities among different billboards. Formally, the transition probability from r_i to r_j, i.e., $p(\overrightarrow{r_i r_j})$, can be calculated as follows:

$$p(\overrightarrow{r_i r_j}) = |\mathcal{TB}_{r_i \to r_j}| / |\mathcal{TB}_{r_i}|, \tag{4}$$

where $|\mathcal{TB}_{r_i \to r_j}|$ represents the number of trajectories sequentially passing through r_i and r_j, and $|\mathcal{TB}_{r_i}|$ denotes the number of trajectories covering r_i. For the ease of exposition, we adopt a graph representation $\mathcal{G} = \{\mathcal{R}, E, W\}$ to characterize association relationship among billboards, where a node set $\mathcal{R}$ denotes the involved billboards, an edge set E represents the transition relationship between any two billboards, e.g., $e_{i,j} = r_i \to r_j$, and weights W are associated transition probabilities, such as $w_{i,j} = p(\overrightarrow{r_i r_j})$. Note that as users can move either from r_i to r_j or from r_j to r_i, $\mathcal{G}$ is a directed graph. Hereafter, we will refer to the terms "billboard" and "node" interchangeably.

Afterwards, we will build our billboard advertising influence diffusion model. For the sake of illustration, let us start with a simple case that ad query q is being displayed only on billboards r_i and r_j ($\mathcal{R}^* = \{r_i, r_j\}$), and the relative transition probabilities are $p(\overrightarrow{r_i r_j})$ and $p(\overrightarrow{r_j r_i})$, respectively. From the perspective of r_j, advertising influence $\mathcal{I}_q^{r_j}$ contains audiences who have visited billboard r_i (i.e., users who have viewed q at r_i will visit billboard r_j with probability $p(\overrightarrow{r_i r_j})$), and we have the same formulation for r_i as well.

Next, the redundant advertising effect existing in r_i and r_j can be calculated as follows:

$$\mathcal{I}_q^{redu} = \mathcal{I}_q^{r_i} * \left[1 - exp(-\beta_{i,j} * p(\overrightarrow{r_i r_j}))\right] + \mathcal{I}_q^{r_j} * \left[1 - exp(-\beta_{j,i} * p(\overrightarrow{r_j r_i}))\right], \tag{5}$$

where $exp(-\beta_{i,j} * p(\overrightarrow{r_i r_j}))$ and $exp(-\beta_{j,i} * p(\overrightarrow{r_j r_i}))$ are *diffusion coefficients*. $\beta_{i,j}$ (or $\beta_{j,i}$) denotes the diminishing return, which is formalized by a Gaussian decay function as below:

$$\beta_{i,j} = exp\left(\frac{-(dist(r_i, r_j) - b_1)^2}{2 * b_2^2}\right), \tag{6}$$

where $dist(r_i, r_j)$ denotes the road network distance between billboard r_i and r_j, and b_1, b_2 are parameters controlling the decay rate. Actually, due to a symmetric property, $\beta_{i,j}$ equals $\beta_{j,i}$. In practice, the effect of advertising influence would decay along with time, which has been verified in References [18, 20]. Considering users' diverse traveling time, we leverage here physical distance as a more general case. In summary, the total advertising influence of r_i and r_j is as below:

$$\mathcal{I}_q^{\mathcal{R}^*} = \mathcal{I}_q^{r_i} + \mathcal{I}_q^{r_j} - \mathcal{I}_q^{redu} = \mathcal{I}_q^{r_i} * exp(-\beta_{i,j} * p(\overrightarrow{r_i r_j})) + \mathcal{I}_q^{r_j} * exp(-\beta_{j,i} * p(\overrightarrow{r_j r_i})). \tag{7}$$

Next, we extend the redundant advertising influence to multiple billboards. Given billboards $\mathcal{R}^*$, $\mathcal{R}^* \subseteq \mathcal{R}$, its total targeted advertising influence $\mathcal{I}_q^{\mathcal{R}^*}$ is calculated as below:

$$\begin{aligned}\mathcal{I}_q^{\mathcal{R}^*} &= \sum_{r_i \in \mathcal{R}^*} \mathcal{I}_q^{r_i} * \left\{1 - \left[1 - exp\left(- \sum_{r_x \in \mathcal{R}^* \backslash r_i} \beta_{i,x} * p(\overrightarrow{r_i r_x})\right)\right]\right\} \\ &= \sum_{r_i \in \mathcal{R}^*} \mathcal{I}_q^{r_i} * \left[exp\left(- \sum_{r_x \in \mathcal{R}^* \backslash r_i} \beta_{i,x} * p(\overrightarrow{r_i r_x})\right)\right] \\ &= \sum_{r_i \in \mathcal{R}^*} \mathcal{I}_q^{r_i} * \prod_{r_x \in \mathcal{R}^* \backslash r_i} exp(-\beta_{i,x} * p(\overrightarrow{r_i r_x})),\end{aligned} \tag{8}$$

where $r_j \in \mathcal{R}^* \backslash r_i$ denotes billboards in $\mathcal{R}^*$ excluding r_i.

3.2 Billboard Rental Price

From the perspective of advertisement exposure opportunity, here we devise a billboard rental price mechanism, instead of using a random simulation. In practical cases, billboard rental price depends on many factors that could contribute to attracting potential consumers.[4] Here, we consider three factors: business popularity, public transit facility, and traffic flow. The business popularity characterizes potential regional commercial value, and public transit facility and traffic flow are used to estimate the scale of audience from different views.

(1) Business Popularity. The business popularity represents commercial prosperity and potential business opportunities. It is a positive factor for billboard rental pricing, as it can potentially attract audiences. Formally, we partition an urban region into a set of grids $\mathcal{D} = \{d_1, d_2, \ldots, d_m\}$ and count the number of commercial POIs (e.g., shopping mall, etc.) located in each grid $\mathcal{N}(d_i), 1 \leqslant i \leqslant m$. To normalize this measurement, we adopt a function $\Psi(x_i)$ as follows:

$$\Psi(x_i) = \frac{x_i}{Max\{x_i | 1 \leqslant i \leqslant n\}}, \tag{9}$$

where x_i is a discrete variable and $\Psi(x_i) \in [0, 1]$. And then each grid d_i's business popularity can be calculated as $\Psi(\mathcal{N}(d_i))$. Note that as one road segment r_i may be partially located in more than one grid, e.g., $\mathcal{D}_{r_i}$, for each road segment r_i, we average all its covered grids' business popularity: $\mathcal{P}_1(r_i) = \frac{1}{|\mathcal{D}_{r_i}|} \sum_{d_i \in \mathcal{D}_{r_i}} \Psi(\mathcal{N}(d_i))$.

(2) Public Transit Facility. This factor implicitly represents the potential traffic of audiences, i.e., billboard impression. We consider three elements to evaluate this metric: the number of buses passing r_i, the number of bus stations located at r_i, and the minimum distance between r_i and available subway stations, which are denoted by $\varphi_{r_i}^1$, $\varphi_{r_i}^2$, and $\varphi_{r_i}^3$, respectively. Specifically, the first two elements are positive for billboard impression, while the last one has a negative effect. By utilizing the above-mentioned normalization function $\Psi()$, we formalize this measurement as $\mathcal{P}_2(r_i) = 1/3 * [\Psi(\varphi_{r_i}^1) + \Psi(\varphi_{r_i}^2) - \Psi(\varphi_{r_i}^3)]$.

(3) Traffic Flow. This measurement obtained from trajectory history $\mathcal{TB}$ can be regarded as samples of the whole traffic flow over r_i, i.e., $fw(r_i)$. Over each road segment r_i, its normalized metric can be computed as: $\mathcal{P}_3(r_i) = \Psi(fw(r_i))$

Finally, each billboard r_i's rental price is formulted by combining all these three type of relative factors:

$$C(r_i) = B_0 * (\mathcal{P}_1(r_i) + \mathcal{P}_2(r_i) + \mathcal{P}_3(r_i)), \tag{10}$$

where B_0 is a base ratio that can be adjusted according to different application requirements.

[4] http://www.lamar.com.

3.3 Problem Definition and Analysis

Definition 1. TOAR Problem. Given an ad query $q = \overrightarrow{\gamma} : \{\gamma_1, \gamma_2, \ldots, \gamma_m\}$, and a set of potential billboards $\mathcal{R} = \{r_1, r_2, \ldots, r_n\}$, the TOAR problem is to search a subset of billboards: $\mathcal{R}^* \subseteq \mathcal{R}$, toward the goal of achieving a maximum targeted advertising influence $\mathcal{I}_q^{\mathcal{R}^*}$ under the specified budget constraint C_{max}, such that $\sum_{r \in \mathcal{R}^*} C(r) \leqslant C_{max}$. Formally, the combinatorial optimization TOAR problem is formalized as follows:

$$\begin{cases} arg\ max_{\mathcal{R}^*} \sum_{r_i \in \mathcal{R}^*} \mathcal{I}_q^{r_i} * \prod_{r_x \in \mathcal{R}^* \setminus r_i} exp(-\beta_{i,x} * p(\overrightarrow{r_i r_x})) \\ S.t. : C(\mathcal{R}^*) \leqslant C_{max} \end{cases}. \tag{11}$$

In the following, we analyze the complexity of our TOAR problem in detail. By reducing the classical **Budgeted Maximum Coverage (BMC)** problem [8], it can proved that our problem is NP-hard. So, there is no polynomial time approach available solving this problem, and we will not be concerned with algorithms giving a global optimal solution but near-optimal solutions. More importantly, as involving a high number of decision variables, i.e., thousands of candidate billboards in citywide settings, our TOAR problem is a large-scale optimization problem. In practice, to tackle the large-scale optimization problem, many commonly used methods, such as **Particle Swarm Optimization (PSO)** and the **Differential Evolution (DE)** algorithm, usually cannot adequately explore the solution space and fail to find a good near optimal solution. Such an issue, typically referred to as the "curse of dimensionality," indicates that the solution space of a large-scale problem grows exponentially with the increase of its dimension.

Moreover, compared with the BMC problem, our problem is more complicated as (1) targeted advertising advertising influence $\mathcal{I}_q^r$ varies with different ad queries, instead of constant value; (2) the two-way mobility association among billboards complicates the total targeted influence calculation. Specifically, when sequentially determining billboards, both the newly selected billboard's influence and already determined billboards' influence might be affected; and (3) with the increasing number of determined billboards, the whole targeted ad influence is non-monotonic but might decrease due to the reinforcement of the redundant advertising effect.

Lemma 3.1. *Targeted billboard advertising influence $\mathcal{I}_q^{\mathcal{R}^*}$ is non-monotonic.*

Proof. Consider two subsets of billboards $\mathcal{R}_1^*$ and $\mathcal{R}_2^*$, where $\mathcal{R}_1^* \subseteq \mathcal{R}_2^*$. For simplicity, we assume that $\mathcal{R}_2^* = \mathcal{R}_1^* \bigcup r_k$, and $r_k \notin \mathcal{R}_1^*$. Then, we have

$$\mathcal{I}_q^{\mathcal{R}_1^*} = \sum_{r_i \in \mathcal{R}_1^*} \mathcal{I}_q^{r_i} * \prod_{r_x \in \mathcal{R}_1^* \setminus r_i} \mathcal{X}_{i,x}, \tag{12}$$

Note that, for the ease of exposition, the relative diffusion coefficient $exp(-\beta_{i,x} * p(\overrightarrow{r_i r_x}))$ is represented as $\mathcal{X}_{i,x}$.

Thus, targeted advertising influence of subset $\mathcal{R}_2^*$ could be calculated as

$$\mathcal{I}_q^{\mathcal{R}_2^*} = \underbrace{\sum_{r_i \in \mathcal{R}_1^*} \mathcal{I}_q^{r_i} * \prod_{r_x \in \mathcal{R}_1^* \setminus r_i} \mathcal{X}_{i,x}}_{\mathcal{I}_q^{\mathcal{R}_1^*}} * \mathcal{X}_{i,k} + \mathcal{I}_q^{r_k} * \prod_{r_x \in \mathcal{R}_1^*} \mathcal{X}_{k,x}. \tag{13}$$

$$\mathcal{I}_q^{\mathcal{R}_2^*} - \mathcal{I}_q^{\mathcal{R}_1^*} = \underbrace{\sum_{r_i \in \mathcal{R}_1^*} \mathcal{I}_q^{r_i} * \prod_{r_x \in \mathcal{R}_1^* \setminus r_i} \mathcal{X}_{i,x}}_{\mathcal{I}_q^{\mathcal{R}_1^*}} * (\mathcal{X}_{i,k} - 1) + \mathcal{I}_q^{r_k} * \prod_{r_x \in \mathcal{R}_1^*} \mathcal{X}_{k,x} \tag{14}$$

However, there is no guarantee that the above equation Equation (14) is not less than 0, due to diverse billboard characteristics, advertising topic, and mobility transition relationship. Thus, we can achieve Lemma 2. □

4 PROPOSED APPROACHES

To effectively solve the high-dimensional problem, it is a natural way to take the idea of divide-and-conquer strategy. Basically, it first decomposes the original problem into a set of smaller and simpler subcomponents and then separately solves the individual subcomponents. In the section, following the practice, in the work, we first devise a graph embedding-based problem decomposition framework to decompose the original problem into several subproblems. Based on it, we propose two approaches to achieve the desired optimal solution, i.e., a master–slave-based sequential optimization algorithm TOAR-MSS, and a cooperative co-evolution-based optimization algorithm TOAR-CC. The reason we devise these two different approaches is that we want to explore the problem-solving from different perspectives, i.e., sequential construction and evolutionary search. Next, we will explain them in detail.

4.1 Graph Embedding-based Problem Decomposition

Generally, many *a priori* problem decomposition methods, e.g., splitting-into-halt decomposition, random grouping decomposition, and so on, have been proposed to accommodate specific problem settings [29]. In practice, the optimization performance is potentially sensitive to the chosen decomposition strategies, especially for those problems containing interdependencies between any two decision variables. In essence, it is desirable to find a suitable decomposition strategy, where the interdependencies among different subcomponents are minimal.

Thinking back our studied TOAR problem, there exist direct and indirect interactions, i.e., underlying transition relationship, between the involved nodes in graph representation $\mathcal{G}$. Taking the characteristics into account, we devise a graph embedding-based problem decomposition strategy. Specifically, it first utilizes the graph embedding technique to learn the low-dimensional vector representation of graph $\mathcal{G}$ and then directly adopts the existing methods, e.g., a k-means algorithm, to cluster the involved nodes into different subcomponents. In this way, the nodes (decision variables), which are strongly interdependent, i.e., associated with high transition probabilities, would be grouped into the same subcomponents; otherwise, they will be assigned into different ones.

Concretely, in our problem setting, the interdependence between candidate nodes directly focuses on the latent mobility transition probability, i.e., edge weight $w_{i,j}$. Thus, we just need to capture the first-order proximity of two nodes, such as r_i and r_j, in the embedding vector space. In other words, the pairwise similarity between node r_i and r_j is calculated by the linked edge weight $w_{i,j}$ and $w_{j,i}$. Based on deep autoencoder [30], we build the graph embedding model accordingly, which is composed of two parts, i.e., the encoder and decoder. To be specific, the encoder, which transforms the candidate nodes into low-dimension vectors, and the decoder, which reconstruct the original connected edges from embedded vectors, are trained concurrently to better maintain the structural information of graph $\mathcal{G}$. The number of input of the autoencoder equals to the scale of nodes contained in $\mathcal{G}$, i.e., $|\mathcal{R}|$, and the number of output is the dimension of embedded low-dimensional vector representation, e.g., χ. Many hidden layers are indispensable to better preserve graph information, and the number of layers and neurons inside a layer is problem specific and varies from one graph structure to another. The optimization objective in the embedding process is given as below.

$$\mathcal{L}_{oss} = \sum_{i,j=1}^{n} w_{i,j} \left\| \mathbf{y}_i^{(\chi)} - \mathbf{y}_j^{(\chi)} \right\|_2^2 = \sum_{i,j=1}^{n} w_{i,j} \|\mathbf{y}_i - \mathbf{y}_j\|_2^2, \tag{15}$$

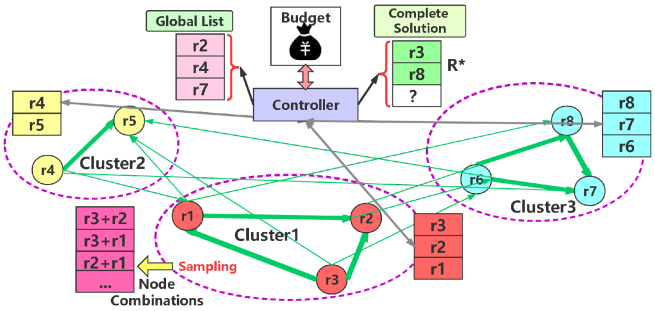

Fig. 2. The workflow of the TOAR-MSS algorithm.

where $\mathbf{y}_i$ denotes the output of encoder for node r_i. When we obtain the low-dimensional vector representations, the k-means algorithm is implemented on these vectors to cluster nodes into a set of disjoint subcomponents: $\{\mathcal{G}_1, \ldots, \mathcal{G}_k\}$, such that $\mathcal{G} = \mathcal{G}_1 \bigcup \mathcal{G}_2 \bigcup \cdots \bigcup \mathcal{G}_k$, and $\forall i \neq j, \mathcal{G}_i \bigcap \mathcal{G}_j = \varnothing$. Figure 2 illustrates a toy example, where eight nodes are grouped into three clusters in different colors, and the thickness of an edge is proportional to its weight.

4.2 Master–Slave Mode-based Sequential Optimization

Based on a master–slave mode, we propose a *greedy sequential optimization* approach, i.e., the TOAR-MSS algorithm, to construct the desired solution. Basically, within each subcomponent $\mathcal{G}_i, 1 \leqslant i \leqslant k$, the greedy sequential probing is implemented to locally construct a partial subsolution $\mathcal{R}_i^*$. Besides, to conquer the intrinsic local optima of greedy sequential optimization, a central controller acted as the master is used to globally coordinate each subcomponent by intercommunicating among all the subcomponents. Finally, we can achieve a desired complete solution $\mathcal{R}^*$ by combining all the partial solutions, i.e., $\mathcal{R}^* = \mathcal{R}_1^* \bigcup \ldots \bigcup \mathcal{R}_k^*$. In the following, we will elaborate it in detail.

4.2.1 The Pipeline of TOAR-MSS. Given an ad query q, all billboards' influence $\mathcal{I}_q^r, r \in \mathcal{R}$, are computed individually. Next, the billboards in each subcomponent are ranked based on the cost performance metric. Formally, this metric formalized by $\mathcal{I}_q^r / C(r)$ denotes the ratio of billboard r's influence over its rental cost. Within each decomposed subcomponent, all the contained billboards are sorted in descending order of their cost performance. The optimization process will sequentially examine all the involved candidate nodes according to this order, instead of blindly traversing. The one with the largest metric is regarded as the "current node" in each subcomponent, and its information will be sent to the master. On the master side, a global list is maintained to record all the current nodes in each subcomponent. And when one current node has been included in $\mathcal{R}_i^*$, the second-largest one in subcomponent $\mathcal{G}_i$ becomes the current node, and its relevant information will be updated in the global list.

At the initial phase, the desired complete solution maintained at master side and all the partial solution in each subcomponent are initialized, i.e., $\mathcal{R}^* = \varnothing$ and $\mathcal{R}_i^* = \varnothing, 1 \leqslant i \leqslant k$. Then, according to the global list, the master selects the top-ϱ current nodes, e.g., $\varrho = 3$, and then the greedy sequential optimization is implemented within their respective subcomponents separately. To be specific, for each selected subcomponent, say, $\mathcal{G}_i$, it attempts to maximize an incremental utility $\Delta\mathcal{I}/\Delta C$ during the solution searching process:

$$\underset{r \in \mathcal{R}_i \setminus \mathcal{R}_i^*}{arg\ max} \left\{ \left[\mathcal{I}_q^{\mathcal{R}^* \cup r} - \mathcal{I}_q^{\mathcal{R}^*} \right] / C(r) \right\}. \tag{16}$$

Following it, we examine all the candidate billboards contained in $\mathcal{G}_i$ and select the one with largest incremental utility to extend its corresponding partial solution $\mathcal{R}_i^*$, i.e., $\mathcal{R}_i^* = \mathcal{R}_i^* \bigcup r$. Note that we combine candidate r with the current discovered complete solution $\mathcal{R}^*$, instead of the partial solution $\mathcal{R}_i^*$. The reason is that we wanted to ensure the effective estimation of utility, i.e., to keep the interdependencies between the subcomponents to a minimum. After handling the ϱ current nodes, the master finally decides the one partial solution with largest incremental utility to extend the complete solution $\mathcal{R}^*$. This process continues until the budget has been exhausted.

However, restricted by the greedy nature, the aforementioned sequential search process might fall into local optima. To avoid it, here we devise a dynamic substitution mechanism to improve the effectiveness of the obtained solution $\mathcal{R}^*$. Briefly speaking, to escape from local optimum, some previously selected billboards might be substituted by other unchosen ones during the optimization process. To be specific, for each billboard r, there are two cases: (1) none of the nodes in r's subcomponent, e.g., $\mathcal{G}_x$, have been selected into $\mathcal{R}^*$, i.e., $\forall r_j \in \mathcal{G}_x, r_j \notin \mathcal{R}^*$, and (2) at least one node in $\mathcal{G}_x$ has been included into $\mathcal{R}^*$, i.e., $\exists r_j \in \mathcal{G}_x, r_j \in \mathcal{R}^*$. Next, we will deal with these two cases separately.

(1) According to Lemma 4.1, for each decomposed subcomponent, it is enough to examine its current node r.

Lemma 4.1. *In the TOAR-MSS algorithm, when handling current node r, where $r \notin \mathcal{R}^* \wedge r \in \mathcal{G}_x$, if $\exists r_i \in \mathcal{G}_x, r_i \notin \mathcal{R}^*$, then r is near optimal among all the uncovered ones in $\mathcal{G}_x$.*

Proof. As nodes are handled in a descending order of their cost performance, we have $[\mathcal{I}_q^r/C(r)] \geqslant [\mathcal{I}_q^{r_j}/C(r_j)]$, where r_j denotes any uncovered nodes in $\mathcal{G}_x$, except r (i.e., $r_j \in \mathcal{R}\backslash\mathcal{R}^* \wedge r \neq r_j$). Then, we have the following approximation: $\mathcal{I}_q^{\mathcal{R}^* \bigcup r} \approx \mathcal{I}_q^{\mathcal{R}^*} + \mathcal{I}_q^r$ due to the weak diffusion association between different subcomponents. In other words, the connected edges between different subcomponents are associated with small weights, i.e., transition probabilities, and have been neglected during variable decomposition. Thus, we have

$$\left\{\left[\mathcal{I}_q^{\mathcal{R}^* \bigcup r} - \mathcal{I}_q^{\mathcal{R}^*}\right]/C(r)\right\} \approx \left[\mathcal{I}_q^r/C(r)\right] \geqslant \left[\mathcal{I}_q^{r_j}/C(r_j)\right]. \tag{17}$$

Considering the redundant advertising effect, the below equation can be derived:

$$\left[\mathcal{I}_q^{r_j}/C(r_j)\right] \geqslant \left\{\left[\mathcal{I}_q^{\mathcal{R}^* \bigcup r_j} - \mathcal{I}_q^{\mathcal{R}^*}\right]/C(r_j)\right\}, \tag{18}$$

$$\left\{\left[\mathcal{I}_q^{\mathcal{R}^* \bigcup r} - \mathcal{I}_q^{\mathcal{R}^*}\right]/C(r)\right\} \geqslant \left\{\left[\mathcal{I}_q^{\mathcal{R}^* \bigcup r_j} - \mathcal{I}_q^{\mathcal{R}^*}\right]/C(r_j)\right\}. \tag{19}$$

So, from the formalized ratio of incremental influence to rental cost, r is near optimal in the uncovered billboards in $\mathcal{G}_x$. □

(2) For the second case, we design a local enumeration procedure within subcomponent $\mathcal{G}_x$ to avoid local optima. To be specific, we harness a local enumeration strategy to dynamically update the already discovered solution $\mathcal{R}^*$. Assume that l nodes in $\mathcal{G}_x$ has been selected into $\mathcal{R}^*$, $\mathcal{G}_x^{\mathcal{R}^*} = \{r_j | r_j \in \mathcal{G}_x \wedge r_j \in \mathcal{R}^*\}$, and $|\mathcal{G}_x^{\mathcal{R}^*}| = l$. Due to the implicit association relationship, it might not be the optimal result by directly adding r into $\mathcal{R}^*$. Thus, we go back to r's subcomponent $\mathcal{G}_x$ and traverse all the possible node combinations of size $l+1$. Obviously, the number of possible node combinations is $C_{|\mathcal{G}_x|}^{l+1}$, where $|\mathcal{G}_x|$ represents the number of nodes contained in subcomponent $\mathcal{G}_x$. We examine each combination and identify the one with the largest incremental utility in terms of gained influence and incurred rental cost. Take Figure 2 as an example. Assume that $\mathcal{R}^*$ includes two nodes, such as $\mathcal{R}^* = \{r_3, r_8\}$. When we examine current node r_2, as $\mathcal{R}^*$ has contained nodes within r_2's subcomponent, i.e., r_3, we invoke the enumeration procedure to find an optimal subsolution of size 2 from possible combinations, i.e., $\{r_3, r_2\}$, $\{r_3, r_1\}$, $\{r_2, r_1\}$, and so on. Supposing

$\{r_2, r_1\}$ has the largest incremental utility, $\mathcal{R}^*$ should be updated to $\mathcal{R}^* = \{r_8, r_2, r_1\}$ accordingly. That is, node r_3, which has been previously included in $\mathcal{R}^*$, is removed.

4.2.2 Pruning Strategies. Owing to the local enumeration operation, our TOAR-MSS algorithm might be time-consuming. To maintain acceptable efficiency, we develop the following pruning strategies to exclude many impossible solutions.

(1) Instead of inspect all the possible enumeration combinations, we pick up a subset of combinations of limited size to further examine cautiously. To be specific, a *random-walk*-based graph sampling technique is adopted. It starts from a random node, say, r_i, and along with directed edges based on probability distribution $\frac{1-p(\overrightarrow{r_i r_j})}{\sum_{r_j \in \texttt{Neighbor}(r_i)[1-p(\overrightarrow{r_i r_j})]}}$ to sample nodes until its length reaches $l+1$, where $\texttt{Neighbor}(r_i) = \{r_j | e_{i,j} = r_i \rightarrow r_j \in E\}$. In this way, the random walk trace can form a billboard combination. This process repeats until a pre-given number of node combinations, i.e., Z, have been obtained. Note that as the factor of edge weight is incorporated during sampling process, its performance could be better than completely random sampling.

(2) Within each subcomponent $\mathcal{G}_x$, to examine billboard combinations of size $l+1$, a benchmark lower bound is built using top-$(l+1)$ nodes in the light of cost performance. Specifically, suppose that the set of selected nodes in cluster $\mathcal{G}_x$ is $\mathcal{G}_x^{\mathcal{R}^*}$ ($\mathcal{G}_x^{\mathcal{R}^*} = \{r | r \in \mathcal{R}^* \wedge r \in \mathcal{G}_x\}$), the lower bound $\mathcal{I}_{wb}$ is represented as below:

$$\mathcal{I}_{wb} = \frac{\mathcal{I}_q^{(\mathcal{R}^* \backslash \mathcal{G}_x^{\mathcal{R}^*} \cup \mathcal{G}_x^{top-(k+1)})} - \mathcal{I}_q^{\mathcal{R}^*}}{C(\mathcal{R}^* \backslash \mathcal{G}_x^{\mathcal{R}^*} \bigcup \mathcal{G}_x^{top-(k+1)}) - C(\mathcal{R}^*)}, \tag{20}$$

where $\mathcal{G}_x^{top-(l+1)}$ denotes the set of top-$(l+1)$ nodes in $\mathcal{G}_x$ in terms of cost performance. Based on it, we provide Lemma 4.2 to prune node combinations that satisfy the criterion with respect to $\mathcal{I}_{wb}$. Actually, as integrated influence calculation (e.g., $\mathcal{I}_q^{\mathcal{R}^*_{-x} \cup \mathcal{G}_x^{l+1}}$) is much more time consuming than simply accumulating up individual influence, i.e., $\sum \mathcal{I}_q^{\mathcal{G}_x^{l+1}}$, TOAR-MSS's search efficiency can be improved significantly.

Lemma 4.2. *Within subcomponent $\mathcal{G}_x$, for any node combination $\mathcal{G}_x^{l+1}$ of size $l+1$, if $\frac{\sum \mathcal{I}_q^{\mathcal{G}_x^{l+1}}}{C(\mathcal{R}^*_{-x} \cup \mathcal{G}_x^{l+1}) - C(\mathcal{R}^*)} \leqslant \mathcal{I}_{wb}$ holds, then $\mathcal{G}_x^{l+1}$ can be directly skipped, where $\mathcal{R}^*_{-x}$ denotes the remaining nodes by excluding $\mathcal{G}_x$'s nodes in $\mathcal{R}^*$.*

Proof. For node combination $\mathcal{G}_x^{l+1}$, its real incremental utility can be calculated as

$$\frac{\mathcal{I}_q^{\mathcal{R}^*_{-x} \cup \mathcal{G}_x^{l+1}} - \mathcal{I}_q^{\mathcal{R}^*}}{C(\mathcal{R}^*_{-x} \bigcup \mathcal{G}_x^{l+1}) - C(\mathcal{R}^*)}. \tag{21}$$

Since our solution searching process is like hill climbing (seeking maximize incremental utility among all the candidate billboards), we have

$$\mathcal{I}_q^{\mathcal{R}^*_{-x} \cup \mathcal{G}_x^{l+1}} - \mathcal{I}_q^{\mathcal{R}^*} \leqslant \mathcal{I}_q^{\mathcal{R}^* \cup \mathcal{G}_x^{l+1}} - \mathcal{I}_q^{\mathcal{R}^*}. \tag{22}$$

As $\mathcal{I}_q^{\mathcal{R}^* \cup \mathcal{G}_x^{l+1}} - \mathcal{I}_q^{\mathcal{R}^*} \leqslant \sum \mathcal{I}_q^{\mathcal{G}_x^{l+1}}$, the following equation holds:

$$\frac{\mathcal{I}_q^{\mathcal{R}^*_{-x} \cup \mathcal{G}_x^{l+1}} - \mathcal{I}_q^{\mathcal{R}^*}}{C(\mathcal{R}^*_{-x} \bigcup \mathcal{G}_x^{l+1}) - C(\mathcal{R}^*)} \leqslant \frac{\sum \mathcal{I}_q^{\mathcal{G}_x^{l+1}}}{C(\mathcal{R}^*_{-x} \bigcup \mathcal{G}_x^{l+1}) - C(\mathcal{R}^*)}. \tag{23}$$

That is, $\mathcal{G}_x^{l+1}$'s real incremental benefit must be less than $\mathcal{I}_{wb}$. So, there is no need to consider combination $\mathcal{G}_x^{l+1}$. □

The pseudo code of the TOAR-MSS algorithm is shown in Algorithm 1.

ALGORITHM 1: TOAR-MSS Algorithm

Input: Graph: $\mathcal{G}$, Ad query: q, Decomposed subcomponent: $\mathcal{G}_i, 1 \leqslant i \leqslant k$, Budget C_{max};
Output: Recommended Billboards: $\mathcal{R}^*$;

```
Initializing R* = ∅ and R*_i = ∅, 1 ⩽ i ⩽ k;
Sort nodes in each subcomponent G_i by cost performance and construct global list;
while ∑_{r∈R*} C(r) ⩽ C_max do
    Take out top-ϱ current nodes from the global list;
    for each selected current node r_i ∈ G_i do
        if ∃ r_j ∈ G_i, r_j ∈ R* then
            Enumerate |G_i^{R*}| + 1 node combinatons in G_i;
            Return the node combination with largest incremental utility;
        else
            Calculate marginal utility: (I_q^{R* ∪ r_i} − I_q^{R*}) / C(r_i);
        end
    end
    Update R* by R*_i with the largest utility;
    Update R*_i and the global list;
end
```

4.2.3 Time Complexity. We discuss the computational complexity of each major module of TOAR-MSS. For simplicity, the size of subcomponents is represented as a fixed value k. The sorting operation costs $k * O(\frac{|\mathcal{R}|}{k} log \frac{|\mathcal{R}|}{k}) = O(|\mathcal{R}| \, log \frac{|\mathcal{R}|}{k})$ to rank the nodes contained in each decomposed subcomponent. Suppose that the average rental price of candidate billboards is C_{ave}, the TOAR-MSS algorithm will be implemented at most $\frac{C_{max}}{C_{ave}}$ rounds. In each round, if one or more nodes that are contained in current node's subcomponent have already been selected into solution $\mathcal{R}^*$, then it will evoke the enumeration procedure. By adopting our designed random-walk-based pruning strategy, its computational overhead is $O(Z * l)$, where Z denotes the preset number of graph sampling, and l represents the average length of node combinations. And to rank all the sampled node combinations is $O(Z * logZ)$. Thus, in worst case, each round takes $O(\varrho * l * Z^2 logZ)$.

4.3 Cooperative Co-Evolution-based Population Optimization

Recently, the most popular Evolutionary Algorithms-based framework to tackle large-scale optimization problem is **Cooperative Co-Evolution (CC)** [21]. Similarly, CC first decomposes the large-scale problem into several smaller and simpler subcomponents. Then each subcomponent is solved by a subpopulation in a round-robin fashion using a chosen optimization method, where each individual in a subpopulation is evaluated in a cooperative way by interacting with the other subcomponents. In this part, based on the CC framework, we propose a population-based approach, namely the TOAR-CC algorithm, to address our problem. In addition, we design two different constraint handling mechanisms to tackle the constraint issue. Compared with the above TOAR-MSS approach, TOAR-CC utilizes the evolutionary algorithm to iteratively search a subsolution within each decomposed subproblem.

4.3.1 Workfolow of the TOAR-CC Algorithm. Generally, the CC framework comprises two serial stages: problem decomposition and multi-cycle subcomponent optimization. Here, we directly use the above-mentioned graph embedding-based decomposition to realize the first stage. In most

of the existing literature, during the subcomponent optimization process, a static decomposition manner is usually adopted, where the decomposed subcomponents remain unchanged over the whole optimization process. It has been shown that, due to the lost of fitness landscape information, the performance of static decomposition will distinctly degenerate for nonseparable problem, i.e., there exit interdependencies between the decision variables [29, 34]. For our TOAR problem, we adopt a dynamical decomposition strategy to alleviate the issue. In other words, the group size is not fixed during the running of CC but dynamically changing. To be specific, based on the learned lower-dimensional embedding vector representation, it conducts k-means clustering in every beginning of the subcomponent optimization cycle by varying the parameter of k in the k-means algorithm. As a result, the decision variables are grouped into different sets of subcomponents in each cycle. By this way, it enables more robust problem decomposition results, and the final performance will be insensitive to the value of parameter k. Formally, in the jth cycle, denoting the ith subcomponent as $\mathcal{G}_i^j$, i.e., $\mathcal{G} = \{\mathcal{G}_1^j, \ldots, \mathcal{G}_k^j\}$, and the best individual in $\mathcal{G}_i^j$ is denoted as $best_i^j$. For each subcomponent, say, $\mathcal{G}_i^j$, one subpopulation with size of PS_i^j is used to optimize it in each cycle.

Next, considering the imbalance feature among subcomponents in terms of their advertising influences and rental prices, it is advisable to pay different attention to each subcomponent. Actually, several contribution-based CC algorithms have been proposed, in which a subcomponent with a higher contribution to the global fitness will be given more computational resources [34]. Along this line of thinking, if one subcomponent $\mathcal{G}_i^j$ has larger utility, then it is likely to be promising area in search space, and more computing resources should be assigned to it during the optimization process. In this work, given one specific ad query q, we exploit the *a priori* knowledge to devise a computing resource predistribution scheme. To be specific, for each subcomponent $\mathcal{G}_i^j$, we estimate the upper bound of its utility $\Lambda(\mathcal{G}_i^j, q)$ as follows:

$$\Lambda(\mathcal{G}_i^j, q) = \sum_{r \in \mathcal{R}_i^j} \frac{\mathcal{I}_q^r}{C(r)}, \tag{24}$$

where $\mathcal{R}_i^j$ denotes the set of nodes contained in $\mathcal{G}_i^j$. Then we specify different scales of subpopulation to each subcomponent in proportions of their estimated upper bounds. In other words, the larger the advertising influence estimation $\Lambda(\mathcal{G}_i^j, q)$ is, the more assigned subpopulation.

Obviously, any one desired solution must satisfy the pre-given budget C_{max}. In fact, with respect to the co-evolutionary constraint handling, it is still in its infancy [1]. Considering our problem characteristics, here we design two different budget constraint handling mechanisms as follows:

(1) *BCHS-I*: During the whole optimization process, all the subpopulations strive to maximize the advertising influence objective regardless of the budget constraint C_{max}. When the multi-cycle optimization stage terminates, a solution repair operation (detailed later) is implemented to calibrate the global solution *gbest*. Basically, it successively removes one node with the lowest cost performance at a time, until *gbest* satisfies the budget constraint.

(2) *BCHS-II*: Different from *BCHS-I*, it decomposes budget C_{max} to the subpopulations before optimization process. Specifically, it normalizes all the decomposed subcomponents' utility estimation, to achieve a distribution vector $\overrightarrow{X} = \{\Lambda(\mathcal{G}_1^j, q), \ldots, \Lambda(\mathcal{G}_k^j, q)\}$. And then, according to the distribution, it randomly chooses a subcomponent $\mathcal{G}_i$ and allocates it a subbudget $C_{max}^{i,j}$, where $\omega * \sum_{r \in \mathcal{R}_i^j} C(r) < C_{max}^{i,j} < \sum_{r \in \mathcal{R}_i^j} C(r)$, $\mathcal{R}_i^j$ denotes the nodes contained in subcomponent $\mathcal{G}_i$, and ω is a regulatory factor. This process continues until the budget C_{max} has been exhausted. In this way, the subcomponents with larger advertising influence estimations will be preferentially allocated budget.

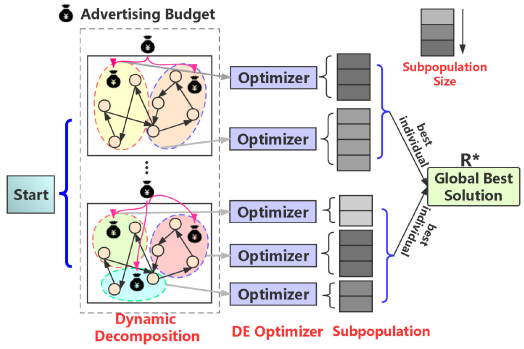

Fig. 3. The workflow of the TOAR-CC algorithm.

With respect to subcomponent optimizer, we utilize the DE [14] as it is a simple yet effective algorithm for global optimization. Based on the reproduction and selection operation (e.g., tournament selection), it selects individuals from the current population to be parents and utilize them to generate the children for the next generation, where the crossover and mutation parameters are set as *cr* and *mr*, respectively. Furthermore, to enhance the search capability of the DE algorithm, we additionally perform a local refinement operation, e.g., variable neighborhood search, to exploit the search subspace in each subcomponent. The neighborhood structures are defined as follows:

(1) $\mathsf{NS}_1()$: For a partial solution, say, the jth individual in ith subpopulation $\mathcal{R}^*_{i,j}$, it randomly select an unchosen node to replace one already selected node.

(2) $\mathsf{NS}_2()$: For $\mathcal{R}^*_{i,j}$, it randomly selects one node and flips its value, i.e., if one node has already been selected in $\mathcal{R}^*_{i,j}$, then it will be discarded; otherwise, it will be included in $\mathcal{R}^*_{i,j}$.

During subcomponent evolutionary, if the fitness of complete solution has not been improved, then the variable neighborhood search will be evoked. In this way, it balances well the exploration and exploitation.

With respect to fitness evaluation, each of its individuals needs to be evaluated by collaborating with the global best solution. At the beginning of the subcomponent optimization stage, we initialize the global best solution *gbest* as a null vector $[0, 0, \ldots, 0]$. For the successive generations, when one evolutionary cycle has finished, it would be compared with the local best solutions $best_i^j$ in each subcomponent $\mathcal{G}_i$, and updated if a better solution has been discovered,

$$gbest = \begin{cases} \left[gbest|best_i^j\right], & if \ \left[gbest|best_i^j\right] > gbest \\ gbest, & otherwise, \end{cases} \tag{25}$$

where $[gbest|best_i^j]$ denotes the overall candidate solution that replaces the corresponding subcomponent of the global best solution *gbest* with $best_i^j$. In this way, the subpopulation interacts with one another through fitness evaluation. In each evolutionary cycle, the optimizer continues to solve every subcomponent, say, $\mathcal{G}_i^j$, until a pre-given stopping criterion threshold has been achieved. Here we adopt a maximum fitness evaluation FE_{max} as the stopping criterion.

In Figure 3, we present the basic workflow of the TOAR-CC algorithm using the *BCHS-II* mechanism. Its pseudo code is outlined in Algorithm 2. Many submodules are described in the following.

4.3.2 Solution Representation. Specifically, each billboard's targeted influence for an ad query q is represented in a vector form, i.e., $\mathcal{I}_q^{\mathcal{R}} = [\mathcal{I}_q^{r_1}, \mathcal{I}_q^{r_2}, \ldots, \mathcal{I}_q^{r_{|\mathcal{R}|}}]$. The desired solution $\mathcal{R}^*$, i.e., *gbest*,

ALGORITHM 2: TOAR-CC Algorithm

Input: Graph: $\mathcal{G}$, Ad query: q, Budget C_{max};
Output: Recommended Billboards: $\mathcal{R}^*$ ($gbest$);
Initializing global best solution $gbest$;
for *each cycle* $j, 1 \leqslant j \leqslant Cyc$ **do**
  $\mathcal{G} = \{\mathcal{G}_1^j, \ldots, \mathcal{G}_k^j\} \leftarrow$ Problem decomposition using k-means by a random value k;
  $\Lambda(\mathcal{G}_i^j, q) \leftarrow$ Estimate each subcomponent $\mathcal{G}_i^j$'s utility upper bound;
  Assign subpopulation and subbudget for $\mathcal{G}_i^j$;
  for *each decomposed subcomponent* $\mathcal{G}_i^j$, **do**
    Initializing local best solution $best_i^j$;
    while $FE \leqslant FE_{max}$ **do**
      $best_i^j \leftarrow$ Optimizer$(\mathcal{G}_i^j, best_i^j, C_{max}^{i,j})$;
    end
  end
  update and repair $gbest$;
end

is defined as a 0-1 indicator vector $\mathbb{U}_{\mathcal{R}^*}$, i.e., $\mathbb{U}_{\mathcal{R}^*} = [u_1, u_2, \ldots, u_{|\mathcal{R}|}]$, where

$$u_i = \begin{cases} 1, & if\ r_i \in \mathcal{R}^* \\ 0, & otherwise. \end{cases} \tag{26}$$

In other words, if r_i has been chosen into $\mathcal{R}^*$, then the ith entry u_i equals 1; otherwise, it is zero, where $0 \leqslant i \leqslant |\mathcal{R}|$.

4.3.3 Fitness Evaluation. For simplicity, we first consider one candidate solution $\mathcal{R}^*$ in limited size, say, $\mathcal{R}^* = \{r_i, r_j, r_k\}$. According to Equation (8), their total ad influence $\mathcal{I}_q^{\mathcal{R}^*}$ is

$$\mathcal{I}_q^{\mathcal{R}^*} = \left[\mathcal{I}_q^{r_i}, \mathcal{I}_q^{r_j}, \mathcal{I}_q^{r_k}\right] * \begin{bmatrix} exp(-\sum_{r_x \in \mathcal{R}^* \setminus r_i} \beta_{i,x} * p(\overrightarrow{r_i r_x})) \\ exp(-\sum_{r_x \in \mathcal{R}^* \setminus r_j} \beta_{j,x} * p(\overrightarrow{r_j r_x})) \\ exp(-\sum_{r_x \in \mathcal{R}^* \setminus r_k} \beta_{k,x} * p(\overrightarrow{r_k r_x})) \end{bmatrix}. \tag{27}$$

For the sake of brevity, if we define diffusion coefficient variable $\mathcal{T}_{i,x} = \beta_{i,x} * p(\overrightarrow{r_i r_x})$, and an exponential function $\mathcal{F}(x) = exp(-x)$, then the above equation could be rewritten as follows:

$$\mathcal{I}_q^{\mathcal{R}^*} = \left[\mathcal{I}_q^{r_i}, \mathcal{I}_q^{r_j}, \mathcal{I}_q^{r_k}\right] * \begin{bmatrix} \mathcal{F}(\sum_{r_x \in \mathcal{R}^* \setminus r_i} \mathcal{T}_{i,x}) \\ \mathcal{F}(\sum_{r_x \in \mathcal{R}^* \setminus r_j} \mathcal{T}_{j,x}) \\ \mathcal{F}(\sum_{r_x \in \mathcal{R}^* \setminus r_k} \mathcal{T}_{k,x}) \end{bmatrix}, \tag{28}$$

where $\sum_{r_x \in \mathcal{R}^* \setminus r_i} \mathcal{T}_{i,x} = [0 \quad 1 \quad 1] * [\mathcal{T}_{i,i} \quad \mathcal{T}_{i,j} \quad \mathcal{T}_{i,k}]^T$, and others could likewise be formalized. After traversing all the involved billboards, all these variables could be recorded in a matrix $\mathcal{T}$. We transform matrix $\mathcal{T}$ into a vector representation, i.e., $[\mathcal{T}_1, \mathcal{T}_2, \ldots, \mathcal{T}_n]^T$, where $\mathcal{T}_i = [\mathcal{T}_{i,1}, \mathcal{T}_{i,2}, \ldots, \mathcal{T}_{i,n}]$ denotes its ith row vector.

Based on the above formulation, our optimization problem can be rewritten as follows:

$$\underset{\mathcal{R}^*}{arg\,max}\ \mathcal{I}_q^{\mathcal{R}} * \left\{\mathcal{F}(\mathcal{P}_{\mathcal{R}^*} * [\mathcal{T}_1, \mathcal{T}_2, \ldots, \mathcal{T}_n]^T)\right\}, \tag{29}$$

where matrix $\mathcal{P}_{\mathcal{R}^*}$ is mathematically represented as follows:

$$\mathcal{P}_{\mathcal{R}^*} = \begin{bmatrix} \mathbb{V}(1) & 0 & \cdots & 0 & 0 \\ & \mathbb{V}(2) & & & \\ \vdots & & \ddots & & \vdots \\ & & & \mathbb{V}(j) & \\ 0 & \cdots & & & \mathbb{V}(n) \end{bmatrix}, \tag{30}$$

where $\mathbb{V}(i)$ is a vector of length n defined as follows:

$$\mathbb{V}(i) = \begin{cases} \mathbb{U}_{\mathcal{R}^*} - \mathbb{I}_i, & if\ r_i \in \mathcal{R}^* \\ [0, 0, \ldots, 0], & otherwise, \end{cases} \tag{31}$$

and $\mathbb{I}_i$ is one unit vector in which the ith entry is 1, and any others are all zeros. In other words, the entries associated with determined billboards are all set to 1, except the ith entry. In essence, our task is to determine the indicator vector $\mathbb{U}_{\mathcal{R}^*}$.

4.3.4 Solution Repair. Moreover, during the subcomponent evolution, the newly discovered solution might violate the budget constraint. Thus, a repair operation is necessary to calibrate these solutions. Basically, we gradually eliminate elements contained in $\mathcal{R}^*$ to meet budget C_{max}. Specifically, by comparing the difference between C_{max} and selected billboards' rental cost, i.e., $|\sum_{r \in \mathcal{R}^*} C(r) - C_{max}|$, we drop the element r whose cost is closest to the calculated difference instead of randomly removing billboards from $\mathcal{R}^*$.

4.3.5 Time Complexity. We discuss the computational complexity of major modules of the TOAR-CC algorithm. During the coevolution process, it requires to optimize all the decomposed subcomponent within Cyc cycles. In each cycle, the computational overhead of the k-means decomposition implementation is $O(|\mathcal{R}| * \chi * k)$, where χ denotes the dimension of embedding vectors. For each decomposed subcomponent $\mathcal{G}_i, 1 \leqslant i \leqslant k$, the optimizer will be conducted FE_{max} generations. During the optimization process, it costs $O(PS_i * \mathcal{R}_i)$ to initialize each subpopulation, where PS_i is the scale of the incumbent subpopulation. The reproduction consumes $O(PS_i^j * PS_i^j * cr)$ and $O(PS_i^j * mr)$ in crossover and mutation operations, and the survivor selection tasks $O(PS_i^j)$.

5 EVALUATION AND DISCUSSION

5.1 Experimental Settings

Datasets. Two real-world datasets collected from Shenzhen and Chengdu, China, respectively are used in our experiments. The first dataset, which contains 425,690 taxi trajectories, is collected from 3,000 taxicabs over 14 days; the second dataset, which contains 3,495,336 trajectories, is collected from 10,000 taxicabs over 20 days. The selected road segments at which the billboards are located are shown in Figure 4(a).

Billboard Rental Price. In this article, we set the base ratio B_0 of our pricing mechanism as 1,000 dollars. The relative distribution of the billboards' rental price in the Chengdu dataset is illustrated in Figure 4(b).

Baseline Algorithms. To the best of our knowledge, there is no work directly related to our studied problem. To evaluate the performance of our proposed approaches, we employ the following algorithms as the baselines for comparison.

- *MCSRS* randomly selects a subset of billboards from $\mathcal{R}$, under the budget constraint C_{max}. This process repeats many times (e.g., 100) and outputs the best result as the final solution.

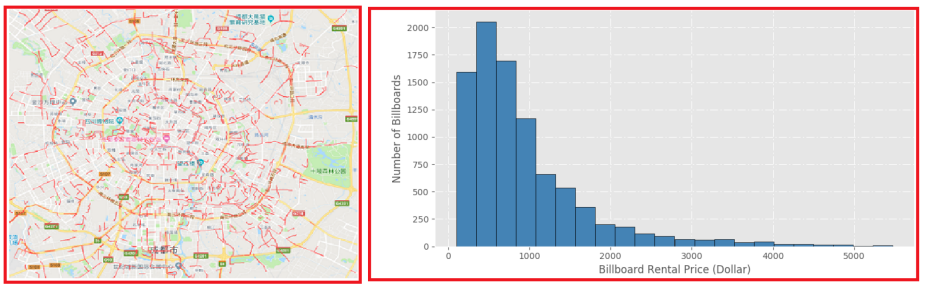

(a) (b)

Fig. 4. The candidate road segments and billboard rental price distribution in Chengdu.

- *NaiveHeur* first arranges all the billboards in the descending order of cost performance. Then, following a descending order, it selects a billboard into $\mathcal{R}^*$ only when the incremental influence by adding the current billboard r into $\mathcal{R}^*$ is positive and otherwise ignored.
- *EAMC* (AAAI 2020) [3] is devised to tackle non-submodular maximization problems with a monotone cost constraint by employing a simple evolutionary algorithm.
- *mCCEA* is a classical and popular CC algorithm [19] that harnesses a dynamic multipopulation strategy to search multiple optima.
- *GloGdy* is a greedy-based optimization that strives to construct the desired solution directly from the whole problem space.
- *B&B* is a branch and bound-based method, and an upper bound estimation is utilized to prune the solution search space [35].

Parameter Settings. The parameter a_0, a_1, and a_2 in exposure strength are set to 1, 10, and 0.04, respectively. With respect to the diffusion coefficient, parameters b_1 and b_2 equal 0 and 1, respectively. The parameter of χ in the graph embedding process is set to 100. With respect to the TOAR-MSS algorithm, the parameter ϱ is set to 3. In the TOAR-CC algorithm, PS is set to the number of candidate billboards, i.e., $|\mathcal{R}|$, FE_{max} is 100, and the parameter k takes values from 100 to 120. And the crossover rate cr and mutation rate mr are set to 0.50 and 0.20, respectively.

5.2 Experimental Results and Analysis

For each technique, we examine its runtime efficiency and the returned advertising influence of the resulting billboard $\mathcal{R}^*$. Every experiment is repeated 10 times, and the average result is reported. First, to comprehensively demonstrate our proposed approaches' performance, we conduct experiments on all involved approaches. The results are present in Figure 5, where $\mathcal{R} = 3000$ and $C_{max} =$ 400,000 dollars.

From the reported experimental results, we observe that our proposed TOAR-CC algorithm achieve the best influence performance, followed by our TOAR-MSS, mCCEA, B&B, EAMC, GloGdy, NaiveHeur, and MCSRS algorithms. Specifically, with respect to the cost-effectiveness, our proposed TOAR-MSS and TOAR-CC algorithms have achieved averagely 4 times of targeted advertising influence than the MCSRS and NaiveHeur. Among all these approaches, the random MCSRS algorithm achieves the worst targeted influence, as it completely ignores the association between billboards, i.e., the redundant advertising effect. Despite the fastest running efficiency, MCSRS's results are unrealistic in practice. Because of utilizing naive heuristics, NaiveHeur yields higher influence performance than MCSRS. However, the roughly sequential comparison makes it quickly hit a performance bottleneck, i.e., trapped into local optima. Compared with the NaiveHeur algorithm, GloGdy strives to achieve an optima by traversing all the candidate elements.

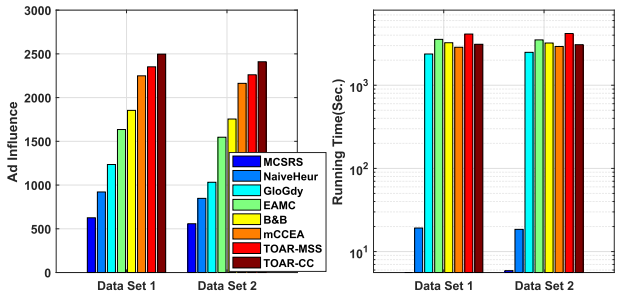

Fig. 5. The experimental results on all involved approaches.

By utilizing a bitwise mutation operation, it enables the ability of the EAMC algorithm to escape from local optima. Thus, its performance significantly outperforms the GloGdy and NaiveHeur algorithm. The B&B algorithm adopt a quasi-enumeration optimization approach with upper bound estimation-based pruning strategies. Its obtains moderate advertising influence performance. By adopting the divide-and-conquer strategy, the mCCEA, TOAR-MSS, and TOAR-CC algorithms achieve better solution quality than the others. Although mCCEA shows stable capability to optimize the ad influence, its performance is still worse than TOAR-MSS and TOAR-CC. Furthermore, the targeted ad influence in dataset 1 is larger than dataset 2; one possible reason is that the road segment distribution and user mobility pattern.

With respect to running time efficiency, as "linear algorithms," the MCSRS algorithm and NaiveHeur algorithm are fastest. Due to traversing the solution space iteratively, the GloGdy algorithm needs more running time to construct the desired optimal solution. Because of the bitwise mutation operation, the running time of the EAMC algorithm expands exponentially with the increase of search space. So the evolution over time is rather slow. Although several pruning strategies have been adopted, the nature of quasi-enumeration makes the B&B algorithm time-consuming. Furthermore, due to local enumeration procedure, TOAR-MSS is time-consuming compared with mCCEA and TOAR-CC. Note that our outdoor advertisement recommendation problem is not a time-intensive task as product recommendation in an E-commerce scenario. For the companies to launch an advertising campaign, they definitely wishes to maximize the influence/product benefit first, even if might take some time to get the optimal result. Therefore, the running efficiency can be acceptable in practical applications.

Varying the Scale of Billboards $\mathcal{R}$: We also investigate the performance of all algorithms when varying the scale of billboards $\mathcal{R}$ from 4,000 to 6,000 with 1,000 increments, where the budget C_{max} remains the same as 400,000 dollars. The experimental results are reported in Figure 6. From it, we make the following observations. First, we can find that generally the performances of the five algorithms are similar to their performances on the above experiments. It also verifies that our proposed approaches maintain good stability with the increase of search space. Second, with the increasing of $\mathcal{R}$, more possible billboards would be examined and chosen. Thus, the returned targeted influence becomes larger. For running efficiency, the linear algorithms, MCSRS and NaiveHeur's, running efficiency is unaffected (they just scan a limited number of billboards), while other algorithms' running times increase accordingly. Note that it is not obvious on the logarithmic axis.

Varying Budget C_{max}: We inspect the performance of all algorithms when varying the promotion budget C_{max} from 300,000, 400,000, to 500,000 dollars, where $|\mathcal{R}|$ is fixed to 3,000. We conduct experiments on these two datasets, respectively, and the experimental results are reported in Figure 7. Actually, with the increasing of promotion budget, the achieved targeted ad influence

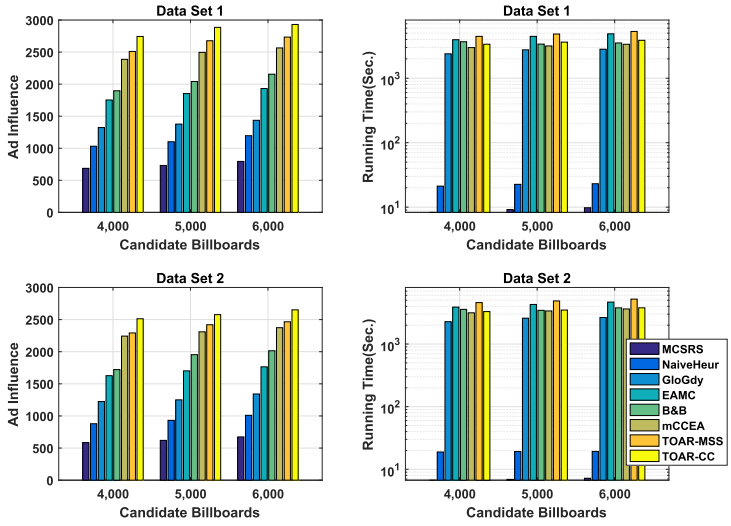

Fig. 6. The experimental results with varying $|\mathcal{R}|$.

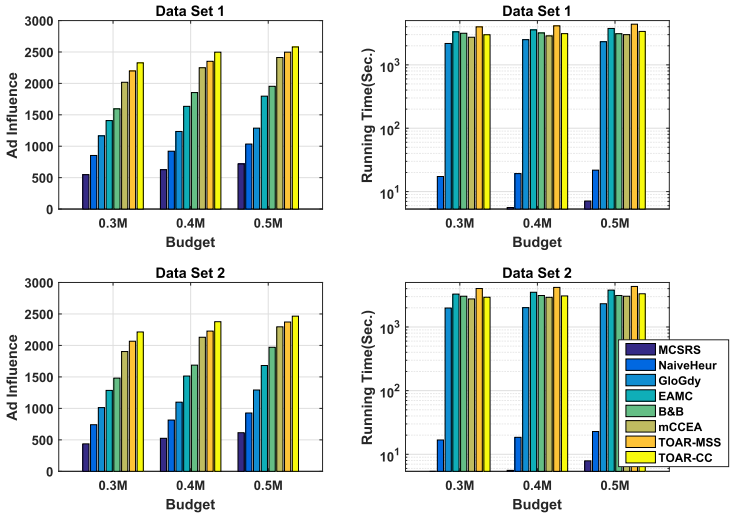

Fig. 7. The experimental results with varying C_{max}.

from all the involved approaches increases accordingly, as more billboards could be rented. Moreover, as adopting a sequential search mode, the running times of NaiveHeur, EAMC, and TOAR-MSS obviously increase more than the other algorithms.

Parameter Sensitivity: We also examine the impact of relevant parameters to the final algorithm performance. First, the impact of parameter k in the graph embedding process is also examined. The candidate billboards are set as 3,000 and the ad budget C_{max} as 400,000. The corresponding results are reported in Figure 8(a) and (b). For space limitations, here we just conduct the comparison experiments on the TOAR-MSS algorithm. Obviously, with the increase of k, the achieved ad influence decreases accordingly. The reason is that when k is larger, it means that more interdependencies will be ignored during the variable decomposition. Moreover, when k

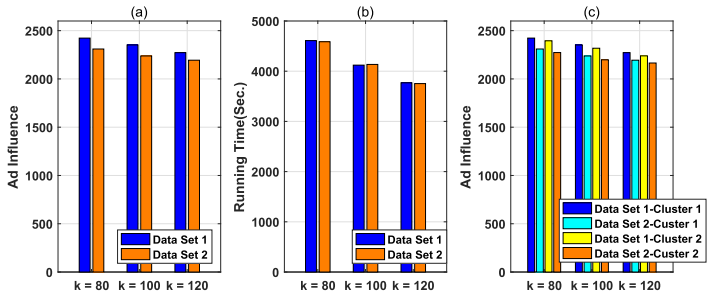

Fig. 8. The impact of graph embedding-based decomposition on TOAR-MSS.

Table 1. The Impact of Budget Allocation on TOAR-CC

Ad Influence	BCHS-I	BCHS-II
Dataset 1	2,426	2,497
Dataset 2	2,389	2,425

becomes large, the number of variables contained in each subcomponent will decrease in an average manner. Thus, the computation time of the enumeration procedure will decrease.

Then we examine the effect of graph embedding technique on the final advertising influence performance via comparing our proposed method with the direct graph clustering. Note that, for the sake of fair comparison, k-means clustering is employed as the direct graph clustering method, and the parameter of k is equal for the same value. The corresponding results are present in Figure 8(c), where "Cluster 1" and "Cluster 2" denote our proposed approach and the direct k-means clustering, respectively. From the reported results, it is found that the graph embedding technique promotes the final performance of targeted advertising recommendation. One potential reason for this is that the graph embedding can well capture the implicit correlation relationship between different nodes, i.e., outdoor billboards. As the scales of decomposed subproblems in these two methods are the same, the running efficiency has no difference between them. Thus, we omit the relevant result here.

Next, we investigate the different budget allocation strategies, i.e., BCHS-I and BCHS-II, in the TOAR-CC algorithm. The problem settings are the same as above. The experimental results are listed in Table 1. From the results, we observe that BCHS-II is better than BCHS-I. The possible reason is that BCHS-II employs a fine-grained allocation strategy during subcomponent evolutionary.

6 CONCLUSION

Based on multi-source urban data, we propose and study a problem of targeted outdoor advertising recommendations. Given a set of billboards and a predefined budget, it strives to response to an ad query and return a subset of billboards maximizing the total targeted advertising influence within budget constraint. By utilizing users' mobility patterns and advertising repetition effects, we build a tailored targeted ad influence model and formalize our problem with a constrained combinatorial optimization problem. To effectively solve it, based on a divide-and-conquer strategy, we develop two approaches, namely the TOAR-MSS and TOAR-CC algorithms. Using two real-world datasets, we conduct extensive experiments to verify the solution effectiveness and search efficiency of our proposed approaches.

REFERENCES

[1] Luis Miguel Antonio and Carlos A. Coello Coello. 2017. Coevolutionary multiobjective evolutionary algorithms: Survey of the state-of-the-art. *IEEE Trans. Evol. Comput.* 22, 6 (2017), 851–865.

[2] Rajeev Batra and Michael L. Ray. 1986. Affective responses mediating acceptance of advertising. *J. Consum. Res.* 13, 2 (1986), 234–249.

[3] Chao Bian, Chao Feng, Chao Qian, and Yang Yu. 2020. An efficient evolutionary algorithm for subset selection with general cost constraints. In *Proceedings of the AAAI Conference on Artificial Intelligence (AAAI'20)*. 3267–3274.

[4] Tao Chen and Kim-Hui Yap. 2013. Discriminative BoW framework for mobile landmark recognition. *IEEE Trans. Cybernet.* 44, 5 (2013), 695–706.

[5] Yi-Cheng Chen, Tipajin Thaipisutikul, and Timothy K. Shih. 2020. A learning-based POI recommendation with spatiotemporal context awareness. *IEEE Transactions on Cybernetics*. DOI: 10.1109/TCYB.2020.3000733

[6] Long Guo, Dongxiang Zhang, Gao Cong, Wei Wu, and Kian-Lee Tan. 2016. Influence maximization in trajectory databases. *IEEE Trans. Knowl. Data Eng.* 29, 3 (2016), 627–641.

[7] Meng Huang, Zhixiang Fang, Shili Xiong, and Tao Zhang. 2019. Interest-driven outdoor advertising display location selection using mobile phone data. *IEEE Access* 7 (2019), 30878–30889.

[8] Samir Khuller, Anna Moss, and Joseph Seffi Naor. 1999. The budgeted maximum coverage problem. *Inf. Process. Lett.* 70, 1 (1999), 39–45.

[9] Amna Kirmani. 1997. Advertising repetition as a signal of quality: If it's advertised so much, something must be wrong. *J. Advert.* 26, 3 (1997), 77–86.

[10] Xiangjie Kong, Zhenzhen Xu, Guojiang Shen, Jinzhong Wang, Qiuyuan Yang, and Benshi Zhang. 2016. Urban traffic congestion estimation and prediction based on floating car trajectory data. *Fut. Gener. Comput. Syst.* 61 (2016), 97–107.

[11] Guoliang Li, Shuo Chen, Jianhua Feng, Kian-lee Tan, and Wen-syan Li. 2014. Efficient location-aware influence maximization. In *Proceedings of the ACM SIGMOD International Conference on Management of Data*. 87–98.

[12] Jianxin Li, Timos Sellis, J. Shane Culpepper, Zhenying He, Chengfei Liu, and Junhu Wang. 2017. Geo-social influence spanning maximization. *IEEE Trans. Knowl. Data Eng.* 29, 8 (2017), 1653–1666.

[13] Yuchen Li, Dongxiang Zhang, and Kian-Lee Tan. 2015. Real-time targeted influence maximization for online advertisements. In *Proceedings of the VLDB Endowment: 41st International Conference on VLDB Endowment, Kohala Coast, Hawaii, 2015 August 31-September 4. 8, 1070–1081*. Research Collection School Of Computing and Information Systems.

[14] Yuan-Long Li, Zhi-Hui Zhan, Yue-Jiao Gong, Wei-Neng Chen, Jun Zhang, and Yun Li. 2014. Differential evolution with an evolution path: A DEEP evolutionary algorithm. *IEEE Trans. Cybernet.* 45, 9 (2014), 1798–1810.

[15] Defu Lian, Yongji Wu, Yong Ge, Xing Xie, and Enhong Chen. 2020. Geography-aware sequential location recommendation. In *In Proceedings of the 26th ACM SIGKDD International Conference on Knowledge Discovery and Data Mining*. 2009–2019.

[16] Defu Lian, Kai Zheng, Yong Ge, Longbing Cao, Enhong Chen, and Xing Xie. 2018. GeoMF++ scalable location recommendation via joint geographical modeling and matrix factorization. *ACM Trans. Inf. Syst.* 36, 8 (2018), 1–29.

[17] Dongyu Liu, Di Weng, Yuhong Li, Jie Bao, Yu Zheng, Huamin Qu, and Yingcai Wu. 2016. Smartadp: Visual analytics of large-scale taxi trajectories for selecting billboard locations. *IEEE Trans. Vis. Comput. Graph.* 23, 1 (2016), 1–10.

[18] Christie L. Nordhielm. 2002. The influence of level of processing on advertising repetition effects. *J. Consum. Res.* 29, 3 (2002), 371–382.

[19] Xingguang Peng, Kun Liu, and Yaochu Jin. 2016. A dynamic optimization approach to the design of cooperative coevolutionary algorithms. *Knowl.-Bas. Syst.* 109 (2016), 174–186.

[20] Pei-Luen Patrick Rau, Jia Zhou, Duye Chen, and Ta-Ping Lu. 2014. The influence of repetition and time pressure on effectiveness of mobile advertising messages. *Telemat. Informat.* 31, 3 (2014), 463–476.

[21] Zhigang Ren, Yongsheng Liang, Aimin Zhang, Yang Yang, Zuren Feng, and Lin Wang. 2018. Boosting cooperative coevolution for large scale optimization with a fine-grained computation resource allocation strategy. *IEEE Trans. Cybernet.* 49, 12 (2018), 4180–4193.

[22] Liang Wang, Zhiwen Yu, Fei Xiong, Dingqi Yang, Shirui Pan, and Zheng Yan. 2019. Influence spread in geo-social networks: A multiobjective optimization perspective. *IEEE Trans. Cybernet.* (2019).

[23] Liang Wang, Zhiwen Yu, Dingqi Yang, Huadong Ma, and Hao Sheng. 2019. Efficiently targeted billboard advertising using crowdsensing vehicle trajectory data. *IEEE Trans. Industr. Inf.* 16, 2 (2019), 1058–1066.

[24] Meng Wang, Hui Li, Jiangtao Cui, Ke Deng, Sourav S. Bhowmick, and Zhenhua Dong. 2016. Pinocchio: Probabilistic influence-based location selection over moving objects. *IEEE Trans. Knowl. Data Eng.* 28, 11 (2016), 3068–3082.

[25] Xiaoming Wang, Xinyan Wang, Geyong Min, Fei Hao, and C. L. Philip Chen. 2020. An efficient feedback control mechanism for positive/negative information spread in online social networks. *IEEE Transactions on Cybernetics*. DOI: 10.1109/TCYB.2020.2977322

[26] Xiaoyang Wang, Ying Zhang, Wenjie Zhang, and Xuemin Lin. 2016. Efficient distance-aware influence maximization in geo-social networks. *IEEE Trans. Knowl. Data Eng.* 29, 3 (2016), 599–612.

[27] Rick T. Wilson, Daniel W. Baack, and Brian D. Till. 2015. Creativity, attention and the memory for brands: An outdoor advertising field study. *Int. J. Advertis.* 34, 2 (2015), 232–261.
[28] Dingqi Yang, Daqing Zhang, Vincent W. Zheng, and Zhiyong Yu. 2014. Modeling user activity preference by leveraging user spatial temporal characteristics in LBSNs. *IEEE Trans. Syst. Man Cybernet.: Syst.* 45, 1 (2014), 129–142.
[29] Zhenyu Yang, Ke Tang, and Xin Yao. 2008. Large scale evolutionary optimization using cooperative coevolution. *Inf. Sci.* 178, 15 (2008), 2985–2999.
[30] Kun Zeng, Jun Yu, Ruxin Wang, Cuihua Li, and Dacheng Tao. 2015. Coupled deep autoencoder for single image super-resolution. *IEEE Trans. Cybernet.* 47, 1 (2015), 27–37.
[31] Chen Zhang, Hao Wang, and Hui Xiong. 2017. An automatic approach for transit advertising in public transportation systems. In *Proceedings of the IEEE International Conference on Data Mining (ICDM'17)*. IEEE, 1183–1188.
[32] Dongxiang Zhang, Long Guo, Liqiang Nie, Jie Shao, Sai Wu, and Heng Tao Shen. 2017. Targeted advertising in public transportation systems with quantitative evaluation. *ACM Trans. Inf. Syst.* 35, 3 (2017), 1–29.
[33] Ping Zhang, Zhifeng Bao, Yuchen Li, Guoliang Li, Yipeng Zhang, and Zhiyong Peng. 2018. Trajectory-driven influential billboard placement. In *Proceedings of the 24th ACM SIGKDD International Conference on Knowledge Discovery & Data Mining*. 2748–2757.
[34] Xin-Yuan Zhang, Yue-Jiao Gong, Ying Lin, Jie Zhang, Sam Kwong, and Jun Zhang. 2019. Dynamic cooperative coevolution for large scale optimization. *IEEE Trans. Evol. Comput.* 23, 6 (2019), 935–948.
[35] Yipeng Zhang, Yuchen Li, Zhifeng Bao, Songsong Mo, and Ping Zhang. 2019. Optimizing impression counts for outdoor advertising. In *Proceedings of the 25th ACM SIGKDD International Conference on Knowledge Discovery & Data Mining*. 1205–1215.
[36] Huanyang Zheng and Jie Wu. 2018. Placement optimization for advertisement dissemination in smart city. *IEEE Transactions on Network Science and Engineering* 7, 1 (2020), 239–252.

Received December 2020; revised July 2021; accepted October 2021